Membrane Potential and Ion Partitioning in an Erythrocyte Using Poisson–Boltzmann Equation

4 AUTHORS, INCLUDING:

Eduardo R A Lima

Rio de Janeiro State University

20 PUBLICATIONS **177** CITATIONS

SEE PROFILE

Frederico W Tavares

Federal University of Rio de Janeiro

132 PUBLICATIONS **1,431** CITATIONS

SEE PROFILE

Membrane Potential and Ion Partitioning in an Erythrocyte Using the Poisson−Boltzmann Equation

Nathalia S. V. Barbosa,[†] Eduardo R. A. Lima,[†] Mathias Boström,[‡] and Frederico W. Tavares*[§,‖]

[†]Programa de Pós-graduação em Engenharia Química, Universidade do Estado do Rio de Janeiro, 20550-013, Rio de Janeiro, Brazil
[‡]Centre for Materials Science and Nanotechnology, University of Oslo, P.O. Box 1048, Blindern, NO-0316 Oslo, Norway
[§]Escola de Química, Universidade Federal do Rio de Janeiro, 21945-970, Rio de Janeiro, Brazil
[‖]Programa de Engenharia Química, COPPE, Universidade Federal do Rio de Janeiro, 21945-970, Rio de Janeiro, Brazil

ABSTRACT: In virtually all mammal cells, we can observe a much higher concentration of potassium ions inside the cell and vice versa for sodium ions. Classical theories ignore the specific ion effects and the difference in the thermodynamic reference states between intracellular and extracellular environments. Usually, this differential ion partitioning across a cell membrane is attributed exclusively to the active ion transport. Our aim is to investigate how much the dispersion forces contribute to active ion pumps in an erythrocyte (red blood cell) as well as the correction of chemical potential reference states between intracellular and extracellular environments. The ionic partition and the membrane potential in an erythrocyte are analyzed by the modified Poisson−Boltzmann equation, considering nonelectrostatic interactions between ions and macromolecules. Results show that the nonelectrostatic potential calculated by Lifshitz theory has only a small influence with respect to the high concentration of K^+ in the intracellular environment in comparison with Na^+.
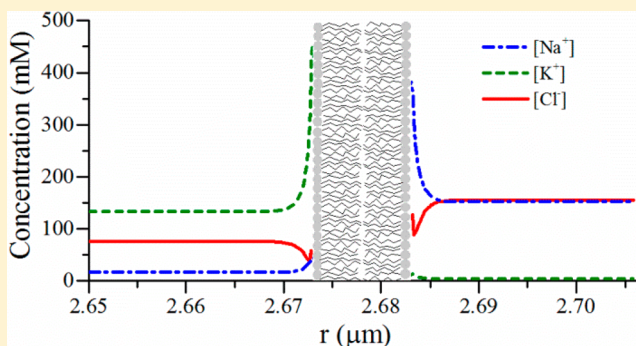
1. INTRODUCTION

Membranes define the external boundaries of biological cells and regulate the molecular transport across these boundaries. Membranes are selectively permeable; i.e., they retain certain compounds and ions within cells while excluding others.[1,2]

The ionic composition of cytosol (intracellular fluid) usually differs greatly from that of the extracellular environment (Table 1). In virtually all cells, the cytosolic concentration of K^+ is much higher than that of Na^+ (the concentration of K^+ is about 30 times higher in cells than in the blood, while the concentration of Na^+ is 10 times lower in cells than in the blood).[1,3]

Table 1. Comparison of Ion Concentrations inside and outside a Typical Mammalian Cell

ion	intracellular concentration[a] (mM)	extracellular concentration[a] (mM)
Na^+	5−15	145
K^+	140	5
Mg^{2+}	0.5	1−2
Ca^{2+}	10^{-4}	1−2
H^+	7×10^{-5} (pH 7.2)	4×10^{-5} (pH 7.4)
Cl^-	5−15	110

[a]From Alberts et al.[2] The cell must contain equal quantities of positive and negative charges. Thus, in addition to Cl^-, the cell contains many other anions like HCO_3^-, PO_4^{3-}, proteins, nucleic acid, etc.

A central issue in molecular biology is that membranes are not merely passive barriers. They include an array of proteins specialized in moving specific organic solutes and inorganic ions across the membrane. In this way, according to the biological literature, ion gradients across membranes are established due to the activity of these specialized membrane proteins. Thus, there is a balance between active and passive transport processes.[1,4] In this context, an active ion transporter stands out: $Na^+K^+ATPase$. This transporter couples phosphorylation−dephosphorylation of an amino acid residue to simultaneous movement of two K^+ ions inward and three Na^+ ions outward across the plasma membrane (the ions are moved against their electrochemical gradients).[3,5] The transmembrane potential that is characteristic of most cells is assigned to the $Na^+K^+ATPase$, once it is an electrogenic transporter, i.e., it creates a net separation of charge across the membrane.[1,3,4]

In the classical theories of physical chemistry of electrolytes, ionic interactions are attributed to electrostatic forces alone, whether among ions or between ions and biomolecules.[6] Therefore, the specific ion or Hofmeister effects are not accounted for by these theories.[7−9] Specific ion effects occur in bulk solutions and at interfaces. In biological systems,

Hofmeister effects are ubiquitous due to the presence of electrolytes and biomolecules in aqueous systems. According to Lo Nostro and Ninham,[9] the concentration at which specific ion effects occur is typically around or above that of physiological solutions.

The specific ion effect has been observed in water dispersions of short chain phospholipids (dioctanoyl-phosphatidylcholine).[10] In this system, an asymmetric distribution of the anions occurs in a finite volume that contains the two phases in equilibrium due to different ion adsorption at the micellar interface. This effect depends on the nature of the electrolyte. Boström et al.[6] studied the same system in order to show theoretically how different anions accumulate in a specific way in the micellar phase. They showed that anions with higher polarizability accumulate in a much higher degree in the phase with phospholipid micelles than anions with lower polarizability. This effect can be quantified taking into account the nonelectrostatic ion binding to micelle surfaces. The same mechanism can be expected to operate in any system of lipids, proteins, or polymers, compartmentalized by a membrane or segregated by equilibrium phase separation due to ion-specific nonelectrostatic (NES) forces.[6]

The partitioning of electrolytes has also been studied in a more realistic biological experiment:[8] several sodium salts were used to analyze the asymmetric partitioning of ions between two equilibrium phases of a surfactant/protein complex (sodium dodecyl sulfate/lysozyme). A reversed Hofmeister series was observed which suggested the importance of specific ion–protein dispersion interactions. Once the two phases are separated, the protein rich phase can either accumulate or exclude most of the present ions, depending on the electrolyte.[8]

These observations indicate that specific ion binding can occur in any finite volume that comprehends two phases in equilibrium, containing different concentrations of lipids, proteins, or polymers. In this way, the specific ion effects can play an important role in ion partitioning that occurs in biological cells; once within the cell, there is a higher protein concentration than in the extracellular environment. A good example of this situation occurs in human erythrocytes.

Human erythrocytes (also denominated red blood cells) are cells responsible for carrying nearly all the oxygen required by the cells from the lungs to the tissues.[1] They are anucleate cells with biconcave discoidal shape in their mature form, free of intracellular organelles. Due to the lack of a nucleus and other organelles, they are considered classic model systems for studying how ions and other compounds in solution go through the plasma membrane.[11]

The cytoplasm of erythrocytes comprises nearly close-packed hemoglobin.[7,11] The distance between the surfaces of neighboring proteins averages only about 20 Å.[12] The hemoglobin is one of the most soluble of all proteins and constitutes more than 98% of erythrocyte protein by mass.[11] It is important to highlight also that hemoglobin is a protein of high surface area.[7]

According to molecular biology, the $Na^+K^+ATPase$ is responsible for maintaining low Na^+ and high K^+ concentrations in the cell relative to the extracellular fluid.[1–3] Electrogenic transport, like $Na^+K^+ATPase$, contributes to the membrane potential that is characteristic of most cells and is essential to the conduction of action potentials in neurons.[1]

The value of the transmembrane potential of human erythrocyte in physiological solution (about −8 to −13.8 mV) has been estimated with different techniques such as microelectrodes,[13,14] fluorescent dyes,[15,16] and measurements of the distribution of chloride ions[11,17,18] and radioactive lipophilic ions.[19]

Considering that both phenomena—active transport by $Na^+K^+ATPase$ and specific ion effects—occur in mammal cells, the aim of this work is to investigate how much the specific ion effects contribute to ion partitioning in erythrocytes. We use Lifshitz theory to quantify the dispersion interactions between ions and macromolecules. In addition, we propose an extra potential that takes into account the energy involved in the difference in chemical potential reference states between the intracellular and extracellular environments and the difference in ion permeability of the erythrocyte membrane and the presence of active transporters at the plasma membrane. To correct the change of the reference state from the intracellular composition to the extracellular environment, we use the Born equation. The system containing an erythrocyte is analyzed using a modified Poisson–Boltzmann theory in Cartesian coordinates.

2. MODELING AND THEORY

In the classical theory, the Poisson–Boltzmann equation takes into account only the electrostatic potential. The inclusion of the dispersion potential between ions and macroparticles in different colloid systems is relevant to explain some phenomena such as adsorption of colloidal particles and surface tension of electrolyte solutions, commonly observed experimentally.[7,20] Aiming at the inclusion of other interactions beyond the electrostatic interactions, we use a modified Poisson–Boltzmann equation[21–23]

$$\varepsilon_0 \nabla \cdot (\varepsilon \nabla \psi) = -e \sum_i z_i c_{i,\infty} \exp\left(-\frac{z_i e\psi + U_i}{k_B T}\right) - \rho_f \tag{1}$$

where ε_0 is the permittivity of the vacuum, ε is the dielectric constant of the medium, $c_{i,\infty}$ is the concentration of ion i (number of ions per unit volume) at an infinitely large distance from the interface (in the bulk solution, $\psi_\infty = 0$), e is the elementary charge, z_i is the charge number of ion i, ψ is the electrostatic potential, k_B is the Boltzmann constant, T is the absolute temperature of the system, ρ_f is the volumetric density of fixed charge, and U_i is the nonelectrostatic energetic contribution of ion i. Nonelectrostatic interactions can be, for example, van der Waals interactions between ion i and the interface and hydration interactions.

The boundary conditions usually associated with eq 1 can be of two types: Dirichlet boundary (potential specified at the boundary) or Neumann boundary (derivative of the potential specified at the boundary). In this work, we apply Neumann boundary conditions, by specifying the surface charge density at $x \to \infty$ and $x \to -\infty$, or $x = x_{surface}$ and $x \to \infty$, or $x \to -\infty$ and $x = x_{surface}$, depending on the system, according to eqs 2 and 3.

$$\left.\frac{d\psi(x)}{dx}\right|_{x\to\pm\infty} = 0 \tag{2}$$

$$\left[\left.\varepsilon\frac{d\psi(x)}{dx}\right|_{interface}\right]\cdot\vec{n} = -\frac{\sigma}{\varepsilon_0} \tag{3}$$

For numerical convenience, we write eq 1 in dimensionless form as

$$\nabla\cdot(\overline{\varepsilon}\,\nabla y) = -\frac{\sum_i z_i c_{i,\infty}\exp(-z_i y - u_i)}{\sum_i z_i^2 c_{i,\infty}} - \overline{\rho}_{\mathrm{f}} \qquad (4)$$

where $y = e\psi/k_{\mathrm{B}}T$ is the dimensionless electrostatic potential; $\overline{\varepsilon}$ is the normalized dielectric constant, that is equal to $\overline{\varepsilon} = \varepsilon/\varepsilon_{\mathrm{w}}$; ε_{w} is the dielectric constant of water at the system's temperature; $u_i = U_i/k_{\mathrm{B}}T$ are the dimensionless nonelectrostatic potentials; and $\overline{\rho}_{\mathrm{f}}$ is the dimensionless volumetric density of fixed charges.

In eq 4, all spatial variables are scaled by κ^{-1}, the Debye length:

$$\kappa^2 = \frac{e^2 \sum_i c_{i,\infty} z_i^2}{\varepsilon_{\mathrm{w}}\varepsilon_0 k_{\mathrm{B}}T} \qquad (5)$$

The Poisson–Boltzmann equation was solved in its dimensionless form (eq 4) by a second order spline finite elements method in a steady one-dimensional Cartesian coordinate system. This method consists of the division of the domain, which defines the problem that we want to model into smaller subdomains. In each of these subdivisions, the dependent variables involved in the problem are approximated by interpolating its values fixed in the boundaries of the subdomain. Thus, the discretization of the differential equation results in algebraic equations whose unknowns are the values of these variables on the boundary of various subdivisions (nodes of the finite elements).[24] The nonlinear term of the Poisson–Boltzmann equation was linearized around the previous iteration value of y at the collocation point of finite element. Thus, the solution should be iterative; i.e., the linearized equations are solved at each iteration and, therefore, the solution of nonlinear equations is obtained after the convergence of consecutive iterations. It is noteworthy that the linear system obtained is a sparse system. The method used to solve the linear algebraic system is a generalized Thomas method for solving heptadiagonal systems.

Considering the equilibrium between the intracellular and extracellular environments, the transmembrane potential between these two compartments is equivalent to the Donnan potential.

The Donnan potential occurs (i) when nonpermeable ions are unequally distributed between two electrolyte solutions separated by a selectively permeable membrane, which allows certain ions to move freely between the two solutions, and (ii) between regions of solution and charged membrane (or charged macromolecules) with a fixed charge interface.[25,26]

In the classical treatment, the Gibbs–Donnan potential is considered to be accompanied by a (discontinuous) potential gap across the membrane surface[27] described by the Nernst equation. Mauro[26] suggested a continuous Donnan potential using the Poisson–Boltzmann equation applied to two regions: one containing fixed charge completely ionized and another one without fixed charge. It is possible to demonstrate that the Donnan potential calculated via the Poisson–Boltzmann equation for remote regions is equal to the difference in potential provided for the Nernst equation.[26,28] In the literature, we can observe two common ways of treating the Donnan potential with the Poisson–Boltzmann equation. One way consists of using Neumann's boundary conditions as in eq 2, together with other conditions: $\psi(x)|_{x\to 0_-} = \psi(x)|_{x\to 0_+}$ and $\nabla\psi(x)|_{x\to 0_-} = \nabla\psi(x)|_{x\to 0_+}$, where the interface is at $x = 0$.[26,27] The other way is using Dirichlet boundary conditions when x

$\to -\infty$, Neumann boundary conditions when $x \to \infty$, and the continuity conditions for $\psi(x)$ and $\nabla\psi(x)$.[29,30] The value of the electrostatic potential in $x \to -\infty$ is considered equal to zero.

In this work, the modified Poisson–Boltzmann equation is solved for both environments (intracellular and extracellular) simultaneously, using regularization functions in order to ensure continuity and to eliminate possible numerical problems. These regularization functions were applied to express the volumetric density of fixed charge, the non-electrostatic energetic contribution of ions, and the dielectric function between intracellular and extracellular environments.

The use of a regularization function to describe volumetric density of fixed charge is a strategy to ensure that the Gibbs–Donnan potential automatically arises from the resolution of the Poisson–Boltzmann equation, solving only one equation for the system.

Regularization functions are used to join two different functions of the same independent variable. This methodology is important when we use the Poisson–Boltzmann equation for two environments simultaneously, in which we can obtain different responses in each compartment. The regularization function is used to generate a continuous function over the entire range of the spatial variable.[31]

We use a hyperbolic tangent function as the regularization function. We consider two generic functions $g(x)$ and $h(x)$, such that

$$f(x) = \begin{cases} g(x), & \text{for } x \leq x^* \\ h(x), & \text{for } x > x^* \end{cases} \qquad (6)$$

where $f(x)$ is a discontinuous function. In order to reconcile the two solutions and turn the function into a continuous function $F(x)$, we apply the following equation

$$F(x) = \nu(x)h(x) + [1 - \nu(x)]g(x) \qquad (7)$$

where

$$\nu(x) = \frac{1 + \tanh\left(\frac{x - x^*}{\eta}\right)}{2} \qquad (8)$$

The parameter η is related to the smoothness of the curve. High values of η generate smoother curves, while low values generate stiff curves.

2.1. van der Waals Dispersion. The NES potential corresponds to the van der Waals dispersion interactions obtained from Lifshitz theory.[32] In Cartesian coordinates, the expression used to calculate U_i is[7,32,33]

$$U_i = -\frac{B_i}{x^3}, \qquad \text{for } x \geq r_i \qquad (9)$$

where x is the perpendicular distance from the center of the ion i to the interface and B_i is the dispersion interaction coefficient of ion i, obtained from Lifshitz theory:

$$\frac{B_i}{k_{\mathrm{B}}T} = \frac{\alpha_i(0)}{4\varepsilon_{\mathrm{w}}(0)}\left[\frac{\varepsilon_{\mathrm{m}}(0) - \varepsilon_{\mathrm{w}}(0)}{\varepsilon_{\mathrm{m}}(0) + \varepsilon_{\mathrm{w}}(0)}\right] + \frac{h}{4\pi k_{\mathrm{B}}T}$$
$$\int_{\nu_{\min}}^{\infty}\frac{\alpha_i(\nu)}{\varepsilon_{\mathrm{w}}(\nu)}\left[\frac{\varepsilon_{\mathrm{m}}(\nu) - \varepsilon_{\mathrm{w}}(\nu)}{\varepsilon_{\mathrm{m}}(\nu) + \varepsilon_{\mathrm{w}}(\nu)}\right]\mathrm{d}\nu \qquad (10)$$

where $\alpha_i(0)$ and $\alpha_i(\nu)$ are the effective polarizabilities in water of ion i at frequencies 0 and ν, respectively, h is Planck's constant, $\nu_{\min} = 2\pi k_{\mathrm{B}}T/h$ is the first nonzero frequency, and

$\varepsilon_j(0)$ and $\varepsilon_j(\nu)$ are the dielectric constants of j at frequencies 0 and ν, respectively. The subscript j can be w for water and m for the macroparticle.

In order to calculate B_i, one needs to know how the effective polarizabilities of ions and the dielectric constants for the macroparticle and the solvent vary with frequency. The polarizability and dielectric constant of a molecule at a frequency ν can be expressed by the harmonic-oscillator model[7,32,33]

$$\alpha(\nu) = \frac{\alpha(0)}{1 + (\nu/\nu^{I})^2} \quad (11)$$

$$\varepsilon(\nu) = 1 + \frac{n^2 - 1}{1 + (\nu/\nu^{I})^2} \quad (12)$$

where n is the refractive index for the sodium D line. The ionization frequency ν^{I} of ions in aqueous solution can be estimated from the free energy of hydration of ions.[32]

2.2. Born Correction Contribution. In situations where two different liquid phases in equilibrium exist in the presence of electrolytes, special attention must be given to reference states. The total environment effect on the transfer of an ion from a finite concentration in one liquid phase to a similar concentration in another phase takes into account two main contributions. One results from a difference in ion–ion interactions in the two solvents, while the other one results from a difference in ion–medium interactions. In implicit models, different environments are characterized mainly by their dielectric response, so both medium effect contributions should largely depend on the dielectric constant. In this way, the Born term correction can be used to capture the effects of ion–medium interactions due to the change in the dielectric constant[34,35]

$$\frac{\Delta G_i^{\mathrm{ex,Born}}}{k_\mathrm{B}T} = \frac{e^2 z_i^2}{8\pi k_\mathrm{B}T\varepsilon_0}\left[\frac{1}{\varepsilon_{\mathrm{mix}}} - \frac{1}{\varepsilon_{\mathrm{ref}}}\right]\frac{1}{r_{\mathrm{B},i}} \quad (13)$$

where $\Delta G_i^{\mathrm{ex,Born}}$ is the energy of transfer of an ion i with Born radius $r_{\mathrm{B},i}$ from an environment with dielectric constant $\varepsilon_{\mathrm{ref}}$ to another one with $\varepsilon_{\mathrm{mix}}$. The subscript ref indicates the solution chosen as a reference state.

The Born energy is equivalent to the electrostatic contribution for the solvation energies. This excess free energy is found by discharging a sphere (represented by an ion) in the first environment, transferring this neutral sphere, and then charging up this sphere in the other environment.[36]

Considering the problem studied here, if the extracellular solution is chosen as the reference state, we need to correct the change of the reference state from the intracellular composition to extracellular solution.

2.3. Erythrocyte Model. The main assumptions used in the model proposed to emulate an erythrocyte are the following:

(a) Temperatures are equal to 310.15 K (same temperature in both sides).
(b) Erythrocyte is considered as a sphere with an equivalent radius of 2.673 μm.
(c) The thickness of the plasma membrane plus glycocalyx is equal to 10 nm.
(d) The surface charge density on the outer surface (glycocalyx) is equal to 0.02 C/m².[37]
(e) The surface charge density on the inner membrane surface is equal to that of the outer membrane plus glycocalyx; i.e., the asymmetric distribution of lipids and proteins in cell membranes was not considered.
(f) The intracellular dielectric constant is equal to 65.22.[38]
(g) The extracellular dielectric constant is equal to the aqueous dielectric constant at the system's temperature (considering that more than 90% by mass of the blood is water[39]).
(h) The presence of proteins in the blood is neglected.
(i) Only Na^+, K^+, and Cl^- ions are present.
(j) The plasma membrane is considered as a flat plane.
(k) The average distance between ions and cytoplasm proteins is equal to 5 Å.
(m) Equilibrium between intracellular and extracellular environments.
(n) The Born radii of Na^+, K^+, and Cl^- are considered equal to 1.68, 2.17, and 1.94 Å, respectively.[40]

The bulk concentrations used in the simulation for Na^+, K^+, and Cl^- are shown in Table 2. The sodium and potassium

Table 2. Ionic Concentration in the Model System Containing an Erythrocyte

ion	intracellular concentration (mequiv/L of H_2O)	extracellular concentration (mequiv/L of H_2O)
Na^+	16.5[a]	151.6[a]
K^+	133.7[a]	4.1[a]
Cl^-	75.7[b]	155.7[c]

[a]From refs 41 and 43. [b]From ref 42. [c]According to the principle of electroneutrality in an extracellular environment.

concentrations in the intracellular and extracellular environments as well as intracellular chloride are in accordance with the experimental data obtained by Funder and Wieth[41,42] and Aribi and collaborators.[43] The chloride concentration in the extracellular environment was obtained through the principle of electroneutrality. As we consider only the presence of chloride anion in the extracellular environment, this concentration must be equal to the sum of the concentrations of all cations in the extracellular environment.

On the basis of the principle of electroneutrality, the equivalent protein concentration in the cell was considered equal to 74.5 mequiv/L.

3. RESULTS AND DISCUSSION

The dispersion interaction coefficients between ions and plasma membrane (B_m) and between ions and cytoplasmic protein (B_p) were calculated using Lifshitz theory.[32] Table 3 shows the static dielectric constants, ionization energies, and refractive indices for water, protein, and plasma membrane used

Table 3. Physical Properties for Water, Protein, and Plasma Membrane

physical properties	water	protein	plasma membrane
n^{a}	1.3313[d]	1.6[d]	1.48[d]
$\varepsilon(0)^{b}$	74.16[e]	2.56[f]	5.0[g]
$h\nu^{Ic}$ (10^{12} erg)	20[f]	20[f]	20[f]

[a]Refractive index (sodium D line). [b]Dielectric constant. [c]Ionization energy. [d]From ref 33. [e]From ref 44. [f]From ref 32. [g]From ref 45.

to calculate the dispersion interaction coefficients presented in Table 4.

Table 4. Van der Waals Dispersion Interaction Coefficients between Ions and Plasma Membrane and between Ions and Cytoplasmic Protein at 310.15 K

ion	$B_m{}^a$ (10^{-50} J m^3)	$B_p{}^b$ (10^{-50} J m^3)
Na$^+$	0.257	0.459
K$^+$	1.083	1.918
Cl$^-$	2.076	3.631

^{a}Dispersion interaction coefficients between ions and plasma membrane. ^{b}Dispersion interaction coefficients between ions and cytoplasmic protein.

Using the Poisson–Boltzmann equation with Neumann boundary conditions in a discontinuous system that mimics an erythrocyte immersed in an infinite bath with bulk salt concentrations equal to that of the extracellular medium (Table 2), we obtain a membrane potential equal to −6.88 mV (Figure 1A). This value is lower than (but close to) that
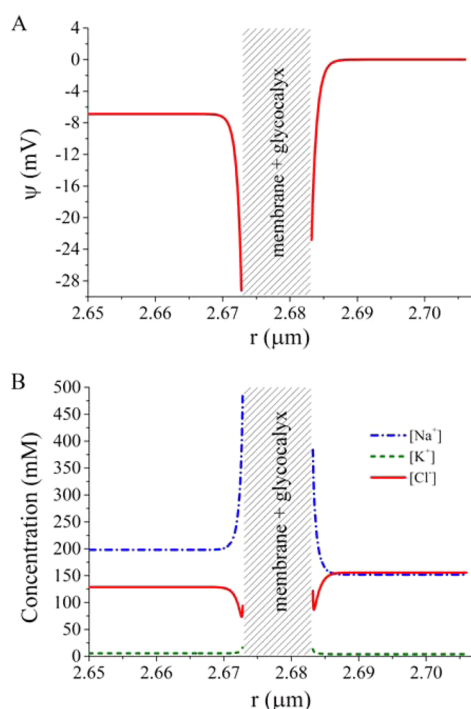

Figure 1. Electrostatic potential profile (A) and ion concentration profile (B) near erythrocyte plasma membrane in a discontinuous system between the intracellular and extracellular environments. Surface charge densities equal to −0.02 C/m^2 and bulk concentration of ions equal to the extracellular concentration shown in Table 2. Plasma membrane plus glycocalyx are represented by hatching.

reported in the literature for an erythrocyte (about −8 to −13 mV),[11,13−19] which can be attributed to the approximations and assumptions used in the model. In this case, we consider the reference bulk concentration of ions equal to their extracellular concentration. In Figure 1B, we show the ion profiles for this system. Near the cell membrane and glycocalyx, there are higher ion concentrations due to the adsorption of ions on these surfaces, including Cl$^-$ (Figure 1B). Although Cl$^-$ and the membrane have like charges, the peak of the Cl$^-$ concentration close to the interface is because of the dispersion interaction

between the ion and plasma membrane. It is worth noting that the value of B_m for Cl$^-$ is higher than the values for the other ions. This effect is best observed at the interface membrane/extracellular solution once the absolute value of the electrostatic potential at the membrane/extracellular interface is smaller than that at the intracellular/membrane interface. We can note that the intracellular concentrations predicted by the model are different from experimental data. As previously mentioned, the intracellular environment has a higher K$^+$ concentration when compared to Na$^+$.[41] The disagreement between computational and experimental data may be occurring due to the difference in reference states between the intracellular and extracellular environments, the difference in ion permeability of the erythrocyte membrane, and/or the presence of active transporters at the plasma membrane.

Analyzing the normalized ion concentration profile within the cell, we can observe that K$^+$ has a slightly greater tendency of concentrating within the cell than Na$^+$ (Figure 2). This is
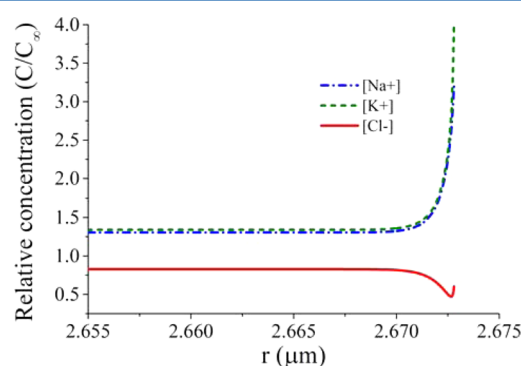

Figure 2. Normalized concentration profile within the cell. K$^+$ has a slightly greater tendency to concentrate within the cell than Na$^+$. Surface charge density equal to −0.02 C/m^2 and bulk concentration of ions equal to the extracellular concentration shown in Table 2.

due to nonelectrostatic interactions. Since there is a large amount of proteins within the cell, K$^+$ that is more polarizable tends to adsorb more to the proteins than Na$^+$. However, nonelectrostatic interactions are not sufficient to explain the higher K$^+$ concentration within the cell observed experimentally. Nevertheless, in this first study, we consider the same overall concentration in the two environments, taking the concentration of extracellular medium as a reference. Had we imposed the bulk concentration of the intracellular medium, we would be imposing the Donnan potential indirectly.

In the literature, this differential ion partitioning of Na$^+$ and K$^+$ is generally attributed to the action of the pump Na$^+$K$^+$ATPase. In order to analyze the potential required to describe experimental ion partitioning, we proposed the inclusion of a potential β in the modified Poisson–Boltzmann equation (eq 1). The algorithm developed for this specific step has an outer loop, in order to reproduce the experimental intracellular concentration values shown in Table 2. For each iteration, new values of β for each ion are obtained until the absolute difference between the intracellular concentration shown in Table 2 and the intracellular concentration calculated for a given estimated β potential is smaller than the tolerance. New values of β for each ion i are calculated according to

$$\beta_i = \ln\left(\frac{c_{i,\infty}}{c_{i,\text{int}}}\right) - z_i y|_{x\to-\infty} - u_i|_{x\to-\infty}$$

(14)

where $c_{i,in}$ is the intracellular concentration of ion i, $y|_{x\to-\infty}$ is the dimensionless electrostatic potential inside the cell at an infinitely large distance from the interface, and $u_i|_{x\to-\infty}$ is the dimensionless nonelectrostatic potential of ion i inside the cell at an infinitely large distance from the interface.

The β potential takes into account the difference in reference states between intracellular and extracellular environments, the difference in ion permeability of the erythrocyte membrane, and short-range hydration forces.

Figure 3A shows the electrostatic potential profile obtained by solving the modified Poisson−Boltzmann equation with the
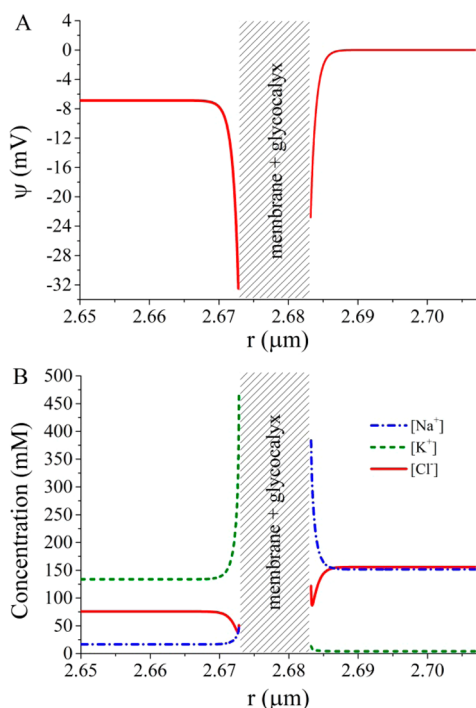

Figure 3. (A) Electrostatic potential profile and (B) ion concentration profile near the erythrocyte plasma membrane in a discontinuous system between the intracellular and extracellular environments considering β potential. Surface charge densities equal to −0.02 C/m² and bulk concentration of ions equal to the extracellular concentration shown in Table 2. Plasma membrane plus glycocalyx are represented by hatching.

inclusion of β potential. Extracellular β potentials for all ions are considered equal to zero. Intracellular values of β for each ion can be seen in Table 5. Comparing the membrane potential in the absence and the presence of β potential, we can observe that it is virtually invariable. Figure 3B shows the ion profiles analyzed in the presence of β potential. As expected, inside the

Table 5. Intracellular Values of β and the Born Term for Na⁺, K⁺, and Cl⁻

ion	nondimensional β potential	$\Delta G_i^{ex,Born}/(k_B T)$	
		$\varepsilon_{in} = 65.22^a$	$\varepsilon_{in} = 57^b$
Na⁺	2.484	0.296	0.651
K⁺	−3.191	0.230	0.503
Cl⁻	0.531	0.257	0.564

[a]Dielectric constant of the intracellular environment equal to 65.22.[38]
[b]Dielectric constant of the intracellular environment equal to 57.[46]

cell, there is more K⁺ than Na⁺, and outside the cell, the inverse occurs.

As previously mentioned, the dielectric constants of the intracellular and extracellular environments are not the same. Then, it is necessary to introduce a correction due to the change of the reference state, which is connected with dielectric constants of both environments. In this context, it is noteworthy that different values of intracellular dielectric constant for normal erythrocytes have been reported in the literature such as 57[46] and 65.22.[38] We analyzed the contribution of this correction in ion−medium interaction for these two different values of intracellular dielectric constant using the Born equation (eq 12). Table 5 shows the values of the Born term for Na⁺, K⁺, and Cl⁻. Comparing the Born correction term for each ion using both intracellular dielectric constant values reported in the literature, it is possible to note that, despite the influence of the dielectric constant in the correction term, the order of magnitude is the same. The values of the β potential and Born term for Cl⁻ are similar with respect to the order of magnitude, suggesting that the difference between the intracellular concentration of Cl⁻ observed experimentally and theoretically in this work can be due to the change of the thermodynamic reference state.

According to Bernhardt and Weiss,[4] under physiological conditions, the net ion movement of K⁺ and Na⁺ in comparison to Cl⁻ across the erythrocyte membrane is very small (about 2 orders of magnitude lower); i.e., the net Cl⁻ permeability across the membrane is larger than the K⁺ and Na⁺ permeability. Therefore, we expect an equilibrium distribution of Cl⁻ between intracellular and extracellular environments, which can be observed comparing β_{Cl^-} with the Born term for this ion. The difference between these terms can be attributed to the consideration of all anions present in the extracellular environment as chloride (including bicarbonates, sulfates, organic phosphates, proteins, etc.), as well as the real value of the intracellular dielectric constant.

If nonelectrostatic interactions between the ions and macromolecules are not explicitly considered in the modified Poisson−Boltzmann equation, the β value for each ion becomes also responsible for expressing the nonelectrostatic potential. The values of β potential for each ion in the system considering or not the nonelectrostatic interactions can be observed in Table 6.

Table 6. Comparison between the β Potential for Na⁺, K⁺, and Cl⁻ Considering or Not the Nonelectrostatic Interactions

ion	β potential (system with NES), nondimensional	β potential (system without NES), nondimensional
Na⁺	2.484	2.475
K⁺	−3.191	−3.227
Cl⁻	0.531	0.464

Comparing the values presented in both columns of Table 6, we can see that the contribution of the nonelectrostatic potential to the ion partitioning of sodium and potassium when compared to β potential is very small (0.4% for Na⁺, 1.1% for K⁺).

We can observe that the contribution of the Born correction term is more evident than nonelectrostatic interaction, at least with respect to Cl⁻. It is worth noting that the magnitude of the Born correction term for Na⁺ and K⁺ is different from β_{Na^+} and

β_{K^+}, respectively. This fact suggests that neither nonelectrostatic interactions nor the Born correction term can explain intracellular K^+ and Na^+ concentrations. Then, the presence of $Na^+K^+ATPase$ is clear.

Bernhardt and Weiss[4] have calculated the ratio between K^+ and Na^+ permeability using the Goldman−Hodgkin−Katz equation. According to their calculation, this ratio was equal to 1.5. Considering β is a term related to ion permeability across the cell membrane, we can calculate the absolute ratio of β_{K^+}/β_{Na^+}. The value obtained is equal to 1.3, close to that predicted by Bernhardt and Weiss. However, we must have in mind that this is an equilibrium calculation and the real cell is not in equilibrium, so this β potential may be related to the extra work done by the active transporters in order to keep the ion concentrations as they are in nature. This extra work is proportional to the permeability of the ions.

The free energy required to move 1 mol of solute across the plasma membrane (toward the extracellular environment to the intracellular) is given by $-RT\ln(C_{ex}/C_{in})$, where R is the universal gas constant, C_{ex} is the extracellular concentration, and C_{in} is the intracellular concentration. This free energy to move an ion i must be equal to $z_iF\delta\psi + RT\delta u_i + RT\delta\beta_i$, where F is the Faraday constant, $\delta\psi$ is the transmembrane potential, δu_i is the difference in transmembrane nonelectrostatic potential, and $\delta\beta_i$ is the difference in transmembrane β potential. This way, we can calculate the free energy required to move 1 mol of ions across the plasma membrane, as presented in Table 7.

Table 7. Free Energy Necessary to Move 1 mol of an Ion across the Plasma Membrane (toward the Extracellular Environment to the Intracellular)

ion	ΔG (kJ/mol)
Na^+	−5.72
K^+	8.99
Cl^-	−1.86

The standard free-energy change for the hydrolysis of ATP is equal to −30.5 kJ/mol. In human erythrocytes, the average concentrations of ATP, ADP, and P_i present in the cytoplasm are equal to 2.25, 0.25, and 1.65 mM, respectively. At pH 7.0 and 25 °C, the free energy change for the hydrolysis of ATP in erythrocytes is equal to −51.8 kJ/mol.[1]

At physiological concentrations of reactants and products, about 11 kcal/mol might be released by the hydrolysis of the terminal phosphate bond in ATP,[47] which corresponds to 46.1 kJ/mol. Sen and Post (1964)[47] found a ratio of active transport cycles of $Na^+K^+ATPase$ equal to $3Na^+:2K^+:(1.16 \pm 0.04)ATP$.

On the basis of the data from Table 7, one transport cycle of $Na^+K^+ATPase$ on a molar basis requires 35.14 kJ (free energy necessary to move 3 mol of Na^+ and 2 mol of K^+ against the electrochemical gradient). In order to compare this energy in terms of ATP, it is necessary to consider the efficiency of the transporter. According to Skou[5] for the transport of Na^+ and K^+ across the plasma membrane, the transporter uses 70−85% of the free energy of the hydrolysis of ATP. Considering 70% efficiency, 50.20 kJ of energy is necessary for the carrying of these ions, equivalent to 0.97 ATP. This value is close to that reported by Sen and Post.[47]

In order to model a continuous system encompassing intracellular and extracellular environments, a peak of volumetric density of fixed charge was estimated and inserted at the interfaces between the electrolyte solutions and plasma membrane to represent each face of the plasma membrane in order to reproduce the electrostatic potential profile of the discontinuous system. The volumetric density of fixed charge at the cytoplasmic face (cytoplasm−membrane interface) shows a minimum value of -1.16×10^8 C/m³, while, at the external face, this value is equal to -9.85×10^7 C/m³.

Figure 4 shows a comparison between continuous and discontinuous systems for the electrostatic potential profile. It is
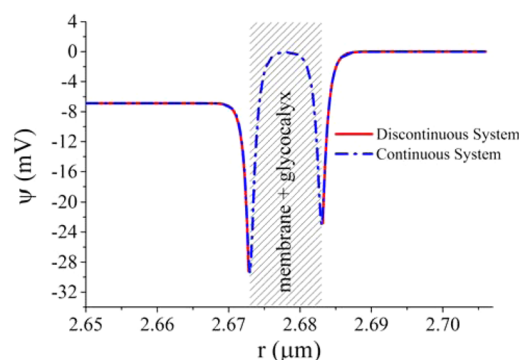

Figure 4. Comparison between continuous and discontinuous systems for the electrostatic potential profile. For the continuous system, the surface charge densities are equal to −0.02 C/m², and for the discontinuous system, the volumetric density of fixed charge at the cytoplasmic face (cytoplasm−membrane interface) shows a minimum value of -1.16×10^8 C/m³, while, at the external face, this value is equal to -9.85×10^7 C/m³. The bulk concentration of ions for both systems is equal to the extracellular concentration shown in Table 2.

noteworthy that the electrostatic potential and concentration profiles within the membrane are not real, being a numerical strategy to ensure the continuity.

The β potential was inserted in the regularization function such that in the extracellular environment this potential for all ions is equal to zero and in the intracellular environment the β potential has a particular value for each ion.

Two situations were analyzed. The first one considers x^*— the parameter used to represent the boundary between the two regions in the regularization function of the β potential—at the interface between the cytoplasm and the plasma membrane, and the other one considers x^* in the middle plane of the plasma membrane.

Figure 5A shows the electrostatic potential profile for the first case. The transmembrane potential is equal to that found for the discontinuous system; nevertheless, the potential of the cytoplasm−membrane interface is lower. However, in the discontinuous system, the potential of the cytoplasm−membrane interface is −32.5 mV, and in the continuous system with x^* at the interface, this potential is equal to −43.0 mV.

In Figure 5B, we observe the ion concentration profile of the first case. We can note that there is an increase of sodium ion concentration near the cytoplasm−membrane interface as well as an increase and a subsequent decrease of the concentration of potassium ion due to the regularization function of the β potential.

Analyzing the same case but for x^* in the middle plane of the plasma membrane, the potential of the cytoplasm−membrane interface is equal to −31.3 mV (Figure 6A), which is closest to that observed in the discontinuous system. The variance in electrostatic potential inside the plasma membrane refers to the impact of the β potential. Therefore, the position of x^* impacts
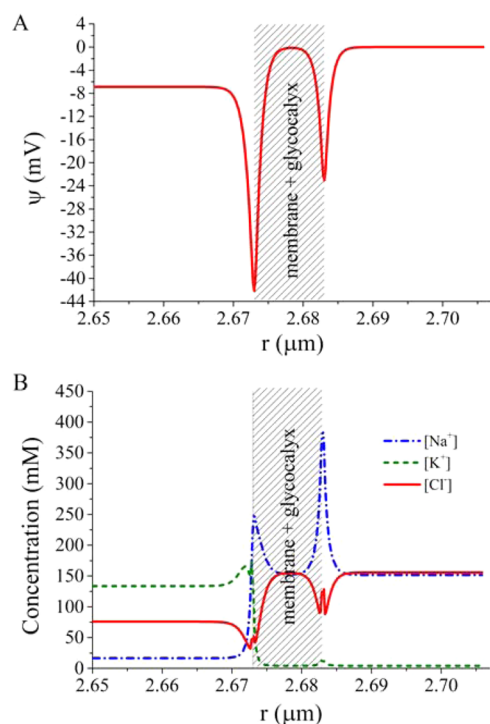
Figure 5. (A) Electrostatic potential profile and (B) ion concentration profile near the erythrocyte plasma membrane in a continuous system between the intracellular and extracellular environments considering x^* relative to the β potential at the cytoplasm−membrane interface. The volumetric density of fixed charge at the cytoplasmic face shows a minimum value of -1.16×10^8 C/m^3, while, at the external face, this value is equal to -9.85×10^7 C/m^3 and the bulk concentration of ions is equal to the extracellular concentration shown in Table 2. Plasma membrane plus glycocalyx are represented by hatching.
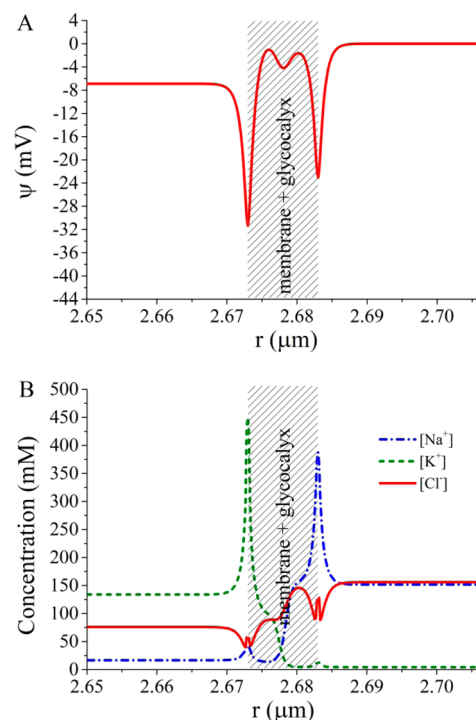

Figure 6. Electrostatic potential profile (A) and ion concentration profile (B) near the erythrocyte plasma membrane in a continuous system between the intracellular and extracellular environments considering x^* relative to the β potential in the middle of the plasma membrane. The volumetric density of fixed charge at the cytoplasmic face shows a minimum value of -1.16×10^8 C/m^3, while, at the external face, this value is equal to -9.85×10^7 C/m^3 and the bulk concentration of ions is equal to the extracellular concentration shown in Table 2. Plasma membrane plus glycocalyx are represented by hatching.

the β potential profiles, which strongly influences the electrostatic potential profile near this point.

Figure 6B presents a similar behavior in comparison with the discontinuous system (Figure 3B), in which there is an increase in the ion concentrations near the membrane interface due to nonelectrostatic interactions with the membrane.

Comparing the ion concentration profiles present in Figures 5B and 6B, we can observe that the latter is more consistent with what is expected, since it presents a peak of K$^+$ concentration near the cytoplasm−membrane interface and a subtle increase in the concentration of Na$^+$ near this interface (Na$^+$ peak in Figure 6B in accordance with the concentration of this ion in the intracellular environment).

4. CONCLUSIONS

The nonelectrostatic potential calculated by Lifshitz theory has only a small influence with respect to the high concentration of K$^+$ in the intracellular environment in comparison with Na$^+$. Despite that the intracellular environment has a larger surface area due to the presence of proteins, it is not sufficient by itself to explain the higher ion partitioning observed experimentally.

The insertion of a Born correction term in the modified Poisson−Boltzmann equation allows analyzing the energy involved in the difference in chemical potential reference states between intracellular and extracellular environments. Although this term cannot explain cation partitioning in erythrocytes, it has a correlation with Cl$^-$ partitioning.

Regarding the membrane potential, the value obtained is lower than that reported in the literature for an erythrocyte. This fact can be attributed to the approximations and assumptions used in the model. The membrane potential in an erythrocyte, according to the literature, is directly related to the concentration of chloride, since this ion has a high permeability across the plasma membrane due to passive ion channels and transporters present. However, the analysis performed in this work considers all other anions present in the system, mainly in the extracellular environment, as chloride.

The electrostatic potential profile analyzed does not include the interior of the plasma membrane which is governed mainly by the dipole potential due to the anisotropic distribution of the lipid headgroup orientation. For the analysis of the potential dipole, it is necessary to use explicit or hybrid techniques.

Two continuous approaches have been proposed for solving a system containing the intracellular and extracellular environments. The advantage of the continuous system involves obtaining the electrostatic potential and concentration profiles of the intracellular and extracellular environments simultaneously using the same algorithm.

■ AUTHOR INFORMATION

Corresponding Author
*E-mail: tavares@eq.ufrj.br.

Notes
The authors declare no competing financial interest.

■ ACKNOWLEDGMENTS

■ REFERENCES

(1) Nelson, D. L.; Cox, M. M. *Lehninger: Principles of Biochemistry*, 5th ed.; W. H. Freeman and Company: New York, 2008.

(2) Alberts, B.; Jonhson, A.; Lewis, J.; Raff, M.; Roberts, K.; Walter, P. *Molecular Biology of the Cell*, 5th ed.; Garland Science: New York, 2008.

(3) Lodish, H.; Berk, A.; Kaiser, C. A.; Krieger, M.; Scott, M. P.; Bretscher, A.; Ploegh, H.; Matsudaira, P. *Molecular Cell Biology*, 4th ed.; W. H. Freeman and Company: New York, 2000.

(4) Bernhardt, I.; Weiss, E. Passive Membrane Permeability for Ions and Membrane Potential. In *Red cell membrane transport in health and disease*; Bernhardt, I., Ellory, J. C., Eds.; Springer: Heidelberg, Germany, 2003; pp 83−119.

(5) Skou, J. C. The Identification of the Sodium-Potassium Pump (Nobel Lecture). *Biosci. Rep.* **1998**, *18*, 155−169.

(6) Boström, M.; Lima, E. R. A.; Biscaia, E. C.; Tavares, F. W.; Lo Nostro, P.; Parsons, D. F.; Deniz, V.; Ninham, B. W. Anion-Specific Partitioning in Two-Phase Finite Volume Systems: Possible Implications for Mechanisms of Ion Pumps. *J. Phys. Chem. B* **2009**, *113*, 8124−8127.

(7) Ninham, B. W.; Lo Nostro, P. *Molecular Forces and Self Assembly*; Cambridge University Press: Cambridge, U.K., 2010.

(8) Lo Nostro, P.; Peruzzi, N.; Severi, M.; Ninham, B. W.; Baglioni, P. Asymmetric Partitioning of Anions in Lysozyme Dispersions. *J. Am. Chem. Soc.* **2010**, *132*, 6571−6577.

(9) Lo Nostro, P.; Ninham, B. W. Hofmeister Phenomena: An Update on Ion Specificity in Biology. *Chem. Rev.* **2012**, *112*, 2286−2322.

(10) Lagi, M.; Lo Nostro, P.; Fratini, E.; Ninham, B. W.; Baglioni, P. Insights into Hofmeister Mechanisms: Anion and Degassing Effects on the Cloud Point of Dioctanoylphosphatidylcholine/Water Systems. *J. Phys. Chem. B* **2007**, *111*, 589−597.

(11) Freedman, J. Membrane Transport in Red Blood Cells. In *Cell Physiology Sourcebook: A Molecular Approach*; Sperelakis, N., Ed.; Academic Press: San Diego, CA, 2001; pp 377−392.

(12) Ponder, E. *Hemolysis and Related Phenomena*; Grune and Stratton: New York, 1948.

(13) Lassen, U. V.; Sten-Knudsen, O. Direct Measurements of Membrane Potential and Membrane Resistance of Human Red Cells. *J. Physiol.* **1968**, *195*, 681−696.

(14) Jay, A. W. L.; Burton, A. C. Direct Measurement of Potencial Difference across the Human Red Blood Cell Membrane. *Biophys. J.* **1969**, *9*, 115−121.

(15) Hoffman, J. F.; Laris, P. C. Determination of Membrane Potentials in Human and Amphiuma Red Blood Cells by Means of Fluorescent Probe. *J. Physiol.* **1974**, *239*, 519−552.

(16) Moersdorf, D.; Egee, S.; Hahn, C.; Hanf, B.; Ellory, C.; Thomas, S.; Bernhardt, I. Transmembrane Potential of Red Blood Cells under Low Ionic Strength Conditions. *Cell. Physiol. Biochem.* **2013**, *31*, 875−882.

(17) Beauge, L. Non-Pumped Sodium Fluxes in Human Red Blood Cells: Evidence for Facilitated Diffusion. *Biochim. Biophys. Acta* **1975**, *401*, 95−108.

(18) Cotterrell, D.; Whittam, R. The Influence of the Chloride Gradient across Red Cell Membranes on Sodium and Potassium Movements. *J. Physiol.* **1971**, *214*, 509−536.

(19) Cheng, K.; Haspel, H. C.; Vallano, M. Lou; Osotimehin, B.; Sonenberg, M. Measurement of Membrane Potentials (ψ) of Erythrocytes and White Adipocytes by the Accumulation of Triphenylmethylphosphonium Cation. *J. Membr. Biol.* **1980**, *56*, 191−201.

(20) Ninham, B. W.; Yaminsky, V. Ion Binding and Ion Specificity: The Hofmeister Effect and Onsager and Lifshitz Theories. *Langmuir* **1997**, *13*, 2097−2108.

(21) Boström, M.; Williams, D. R. M.; Ninham, B. W. Specific Ion Effects: Role of Salt and Buffer in Protonation of Cytochrome c. *Eur. Phys. J. E* **2004**, *13*, 239−245.

(22) Boström, M.; Williams, D. R. M.; Ninham, B. W. Ion Specificity of Micelles Explained by Ionic Dispersion Forces. *Langmuir* **2002**, *18*, 6010−6014.

(23) Boström, M.; Lima, E. R. A.; Tavares, F. W.; Ninham, B. W. The Influence of Ion Binding and Ion Specific Potentials on the Double Layer Pressure between Charged Bilayers at Low Salt Concentrations. *J. Chem. Phys.* **2008**, *128*, 135104.

(24) Dhatt, G.; Touzot, G.; Lefrançois, E. *Finite Element Method*; John Wiley & Sons, Inc.: Hoboken, NJ, 2012.

(25) Krysinski, P.; Ti Tien, H. Membrane Electrochemistry. *Prog. Surf. Sci.* **1986**, *23*, 317−412.

(26) Mauro, A. Space Charge Regions in Fixed Charge Membranes and the Associated Property of Capacitance. *Biophys. J.* **1962**, *2*, 179−198.

(27) Ohshima, H.; Ohki, S. Donnan Potential and Surface Potential of a Charged Membrane. *Biophys. J.* **1985**, *47*, 673−678.

(28) Chein, R.; Chen, H.; Liao, C. Investigation of Ion Concentration and Electric Potential Distributions in Charged Membrane/electrolyte Systems. *J. Membr. Sci.* **2009**, *342*, 121−130.

(29) Ohshima, H. The Donnan Potential-Surface Potential Relationship for a Cylindrical Soft Particle in an Electrolyte Solution. *J. Colloid Interface Sci.* **2008**, *323*, 313−316.

(30) Ohshima, H. Double Layer Interaction between Soft Particles. In *Theory of Colloid and Interfacial Electric Phenomena*; Ohshima, H., Ed.; Elsevier: London, 2006; pp 390−408.

(31) Freitas, T. C.; Quinto, T. C.; Secchi, A. R.; Biscaia, E. C. An Efficient Adjoint-Free Dynamic Optimization Methodology for Batch Processing Using Pontryagin's Formulation. In *22nd European Symposium on Computer Aided Process Engineering*; Bogle, I. D. L., Fairweather, M., Eds.; Elsevier: Amsterdam, The Netherlands, 2012; pp 1297−1301.

(32) Tavares, F. W.; Bratko, D.; Blanch, H. W.; Prausnitz, J. M. Ion-Specific Effects in the Colloid-Colloid or Protein-Protein Potential of Mean Force: Role of Salt-Macroion van der Waals Interactions. *J. Phys. Chem. B* **2004**, *108*, 9228−9235.

(33) Israelachvili, J. N. *Intermolecular and Surface Forces*, 3rd ed.; Academic Press: Burlington, MA, 2011.

(34) Robinson, R. A.; Stokes, R. H. *Electrolyte Solutions*; Dover: New York, 2002.

(35) Chen, C.; Song, Y. Generalized Electrolyte-NRTL Model for Mixed-Solvent Electrolyte Systems. *AIChE J.* **2004**, *50*, 1928−1941.

(36) Dill, K. A. *Molecular Driving Forces: Statistical Thermodynamics in Chemistry and Biology*; Garland Science: New York, 2003.

(37) Donath, E.; Lerche, D. 309 - Electrostatic and Structural Properties of the Surface of Human Erythrocytes. I-Cell-Electrophoretic Studies Following Neuraminidase Treatment. *Bioelectrochem. Bioenerg.* **1980**, *7*, 41−53.

(38) Di Biasio, A.; Cametti, C. On the Dielectric Relaxation of Biological Cell Suspensions: The Effect of the Membrane Electrical Conductivity. *Colloids Surf., B* **2011**, *84*, 433−441.

(39) Feher, J. J. Plasma and Red Blood Cells. In *Quantitative Human Physiology: An Introduction*; Feher, J. J., Ed.; Academic Press: San Diego, CA, 2012; pp 428−436.

(40) Rashin, A. A.; Honig, B. Reevaluation of the Born Model of Ion Hydration. *J. Phys. Chem.* **1985**, *89*, 5588−5593.

(41) Funder, J.; Weith, J. Potassium, Sodium and Water in Normal Human Red Blood Cells. *Scand. J. Clin. Lab. Invest.* **1966**, *18*, 167−180.

(42) Funder, J.; Weith, J. Chloride and Hydrogen Ions Distribution between Human Red Cell and Plasma. *Acta Physiol. Scand.* **1966**, *98*, 234−245.

(43) Aribi, M.; Haddouche, M.; Benyoucef, M.; Taleb, A.; Kendouci-tani, M.; Merzouk, S. A.; Meziane, A. Clinical Evaluation of Lipids, Lipoproteins and Red Blood Cells Sodium and Potassium in Patients with Different Grades of Hypertension. *Clin. Biochem.* **2010**, *43*, 942–947.

(44) Malmberg, C. G.; Maryott, A. A. Dielectric Constant of Water from 0° a 100°C. *J. Res. Natl. Bur. Stand. (U. S.)* **1956**, *56*, 1–6.

(45) Sperelakis, N. *Cell Physiology Source Book: A Molecular Approach*, 3rd ed.; Academic Press: San Diego, CA, 2001.

(46) Gascoyne, P.; Pethig, R.; Satayavivad, J.; Becker, F. F.; Ruchirawat, M. Dielectrophoretic Detection of Changes in Erythrocyte Membranes Following Malarial Infection. *Biochim. Biophys. Acta* **1997**, *1323*, 240–252.

(47) Sen, A. K.; Post, R. L. Stoichiometry and Localization of Adenosine Triphosphate-Dependent Sodium and Potassium Transport in the Erythrocyte. *J. Biol. Chem.* **1964**, *239*, 345–352.